Transcriptional activation of hypoxia-inducible factor-1 (HIF-1) in myeloid cells promotes angiogenesis through VEGF and S100A8

G-One Ahn[a,b,1], Jun Seita[c], Beom-Ju Hong[a], Young-Eun Kim[a], Seoyeon Bok[a], Chan-Ju Lee[a], Kwang Soon Kim[a], Jerry C. Lee[d], Nicholas J. Leeper[d], John P. Cooke[d], Hak Jae Kim[e], Il Han Kim[e], Irving L. Weissman[c], and J. Martin Brown[b]

[a]Division of Integrative Biosciences and Biotechnology, Pohang University of Science and Technology, Pohang, Gyeongbuk 790-784, Korea; [b]Department of Radiation Oncology, [c]Institute for Stem Cell Biology and Regenerative Medicine, and [d]Cardiovascular Institute, Stanford University School of Medicine, Stanford, CA 94305; and [e]Department of Radiation Oncology, Seoul National University College of Medicine, Seoul 110-744, Korea

Edited* by Napoleone Ferrara, University of California, San Diego, La Jolla, CA, and approved January 7, 2014 (received for review October 30, 2013)

Emerging evidence indicates that myeloid cells are essential for promoting new blood vessel formation by secreting various angiogenic factors. Given that hypoxia-inducible factor (HIF) is a critical regulator for angiogenesis, we questioned whether HIF in myeloid cells also plays a role in promoting angiogenesis. To address this question, we generated a unique strain of myeloid-specific knockout mice targeting HIF pathways using human S100A8 as a myeloid-specific promoter. We observed that mutant mice where HIF-1 is transcriptionally activated in myeloid cells (by deletion of the von Hippel–Lindau gene) resulted in erythema, enhanced neovascularization in matrigel plugs, and increased production of vascular endothelial growth factor (VEGF) in the bone marrow, all of which were completely abrogated by either genetic or pharmacological inactivation of HIF-1. We further found that monocytes were the major effector producing VEGF and S100A8 proteins driving neovascularization in matrigel. Moreover, by using a mouse model of hindlimb ischemia we observed significantly improved blood flow in mice intramuscularly injected with HIF-1–activated monocytes. This study therefore demonstrates that HIF-1 activation in myeloid cells promotes angiogenesis through VEGF and S100A8 and that this may become an attractive therapeutic strategy to treat diseases with vascular defects.

Although angiogenesis has been characterized as endothelial cell proliferation and sprouting (1), much of recent evidence suggest that myeloid cells (cells that give rise to monocytes and macrophages) also play an essential part of this process. Many studies have demonstrated that myeloid cells produce various angiogenic factors including vascular endothelial growth factor (VEGF) (2), interleukin 8 (IL-8) (3), basic fibroblast growth factor (bFGF) (4), and Bv8 (5).

Many of these factors such as VEGF (6), IL-8 (7), and bFGF (8) are in fact downstream targets of hypoxia-inducible factor (HIF), a basic helix–loop–helix transcription factor of the Per-ARNT-Sim superfamily. HIF is a heterodimeric complex composed of a constitutively expressed HIF β-subunit and an oxygen-sensitive HIF α-subunit (6), in which all three α-subunits known to date (HIF-1α, -2α, and -3α) are targeted for rapid proteasomal degradation by the von Hippel–Lindau tumor suppressor pVHL, which acts as the substrate recognition component of an E3 ubiquitin ligase complex (9).

HIF has been extensively characterized in cancer cells as a master regulator for hundreds of genes involved in cell survival, adaptation to hypoxia, metabolism, and angiogenesis (6). Previous studies have reported myeloid-specific HIF knockout (KO) mice generated by using LysM as the myeloid promoter, demonstrating the role of HIF in myeloid cells in inflammatory responses (10, 11). For instance, mice deficient for HIF-1α in myeloid cells are more susceptible to the bacterial challenge resulting from defects in ATP generation, which results in impaired intracellular killing of the bacteria in macrophages (10). Mice deficient for HIF-2α in myeloid cells, are on the other hand more resistant to endotoxic shock due to altered chemokine receptor expression on macrophages affecting their chemotactic migration and invasion properties (11). Although these studies have underscored the importance of HIF in myeloid cells for inflammation, it is still poorly understood whether HIF in myeloid cells contributes to angiogenesis.

Here, we generated a unique strain of myeloid-specific KO mice targeting HIF pathways, in which we used the human S100A8 (hS100A8) promoter and found that HIF-1, but not HIF-2, transcriptional activation in myeloid cells can promote new blood vessel formation. S100A8, also known as myeloid-related protein-8, is an intracellular calcium-binding protein whose expression has been detected in myeloid cells (including common myeloid progenitors, granulocytes/macrophage progenitors, monocytes, and granulocytes) but not in hematopoietic stem cells, cells of the lymphoid lineage, erythrocytes, or megakaryocytes (12). By using our unique strain of mice, we found that monocytes, among cells of the myeloid lineage, were the major effector driving the angiogenic effects through HIF-1–activated VEGF and S100A8 production and that these cells were sufficient to promote angiogenesis in matrigel and to improve blood flow in a mouse model of hindlimb ischemia. Based on our findings, we believe that HIF-1 activation in myeloid cells may become a therapeutic strategy to treat various human diseases of abnormal vascularity, such as peripheral arterial disease and diabetic wounds.

Results

Enhanced Angiogenic Phenotypes in Mice Deficient for pVHL in Myeloid Cells. The mice deficient for pVHL in myeloid cells using the hS100A8 promoter (hS100A8Cre + $Vhl^{fl/fl}$) exhibited erythema particularly noticeable in the snouts, paws, ears, and the tail starting from ∼4 wk of age (Fig. 1*A*). Erythema was not observed in wild-

Significance

Here, we are reporting our findings that hypoxia-inducible factor 1 (HIF-1) activation in monocytes promotes neovascularization in matrigel and improves blood flow in hindlimb ischemia through production of vascular endothelial growth factor and S100A8. We found that HIF-1 regulates S100A8 expression specifically in monocytes isolated from our unique strain of transgenic mice targeting HIF pathways.

Author contributions: G-O.A., J.S., N.J.L., J.P.C., H.J.K., I.H.K., I.L.W., and J.M.B. designed research; G-O.A., J.S., B.-J.H., Y.-E.K., S.B., C.-J.L., K.S.K., and J.C.L. performed research; I.L.W. contributed new reagents/analytic tools; G-O.A. and J.S. analyzed data; and G-O.A. wrote the paper.

The authors declare no conflict of interest.

*This Direct Submission article had a prearranged editor.

[1]To whom correspondence should be addressed. E-mail: goneahn@postech.ac.kr.

This article contains supporting information online at www.pnas.org/lookup/suppl/doi:10.1073/pnas.1320243111/-/DCSupplemental.

type (WT) mice not carrying the *Cre*-transgene (Fig. 1*A*) nor in another myeloid-specific *Vhl* KO mouse strain using the LysM promoter (LysMCre + $Vhl^{fl/fl}$; Fig. S1*A*), previously reported by other investigators (13). To test the possibility of whether erythema in our hS100A8Cre + $Vhl^{fl/fl}$ mice (hereafter denoted as "*Vhl* mutant") was due to elevated red blood cells resulting from HIF activation leading to erythropoietin (EPO) production (9), we performed blood cell counts in these animals. We found that there was no significant difference in the red blood cell numbers or hemoglobin levels between the WT and *Vhl* mutant mice (Fig. 1*B*).

We then examined whether erythema was associated with enhanced angiogenesis. To do this, we first performed an antibody array using bone marrow lysates obtained from WT or *Vhl* mutant mice. We observed that there was a significant increase in Vegf protein expression in *Vhl* mutant compared with that in WT mice (Fig. 1*C* and Table S1). Based on the antibody array results, only Vegf and a couple of others including IL-1α and PlGF seemed to show HIF-1 dependency (Tables S1–S3), hence we focused on Vegf protein in the following studies.

To determine whether the increase in Vegf protein would result in increased angiogenesis in *Vhl* mutant mice, we s.c. implanted matrigel plugs (14) and examined vessel formation by immunostaining the matrigel for endothelial cells using CD31 antibodies. We found that there was a significant increase in CD31 area densities in matrigel implanted in *Vhl* mutants compared with that in WT mice (Fig. 1*D*). To investigate VEGF signaling in matrigel of *Vhl* mutant mice in more details, we performed Western blots using matrigel lysates that had been implanted without VEGF supplement (but still supplemented with bFGF). Omitting VEGF supplement still exhibited similar vessel formation in matrigel (Fig. S1*C*). We observed that Vegf and phosphorylated (therefore activated) VEGF receptor-2 (Vegfr-2), the prominent VEGF receptor on endothelial cells (15), were significantly increased in *Vhl* mutant mice compared with WT mice (Fig. 1*E*). Furthermore, increased S100A8 and Hif-1α protein levels were detected in matrigel implanted in *Vhl* mutant mice (Fig. 1*E*). We found no statistical difference in CD11b area densities between WT and *Vhl* mutant mice (Fig. 1*F*), suggesting that monocyte infiltration to matrigel was similar in these mice. In contrast to our *Vhl* mutant mice, such enhanced neovascularization in matrigel was not observed LysMCre + $Vhl^{fl/fl}$ mice (Fig. S1*B*).

We then blocked VEGF–VEGFR2 signaling in the matrigel implanted in *Vhl* mutant mice by injecting DC101, rat anti-mouse Vegfr-2 antibodies. We observed that DC101 significantly abolished blood vessel formation in matrigel in a dose-dependent manner (Fig. S1 *D* and *E*).

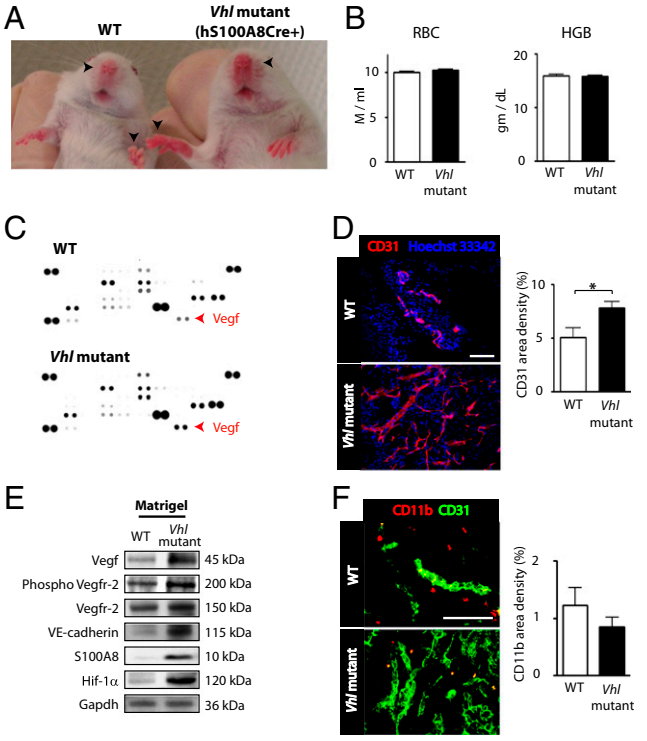

Fig. 1. Enhanced angiogenic phenotypes in mice deficient for pVHL in hS100A8 myeloid cells. (*A*) *Vhl* mutant mice exhibited erythema (black arrowheads) compared with WT mice. (*B*) Red blood cell (RBC) or hemoglobin (HGB) levels in WT ($n = 4$) or *Vhl* mutant ($n = 10$) mice. Data are the mean ± SEM. (*C*) Antibody array analyses of the *Vhl* mutant or WT mice using bone marrow lysates. Note that Vegf levels (red arrowhead) were increased approximately twofold in *Vhl* mutant mice. Quantitative results are shown in Table S1. (*D*) Immunostaining of matrigel implanted in WT or *Vhl* mutant mice for CD31 endothelial cells (red). Hoechst 33342 (blue) was i.v. administered immediately before the matrigel harvest. (Scale bar: 100 μm.) Quantification of CD31 area density is shown in the bar graph. Data are the mean ± SEM ($n = 7$ for WT; n= 18 for *Vhl* mutant mice). *$P < 0.05$ determined by unpaired Student *t* test. (*E*) Western blot of matrigel lysates obtained from *Vhl* mutant or WT mice. (*F*) Immunostaining of matrigel in *D* for CD11b (red) or CD31 (green). (Scale bar and *n* numbers are as in *D*.)

Angiogenic Phenotypes in Mice Deficient for pVHL Require HIF-1 Activation in Myeloid Cells. To determine whether the above angiogenic phenotype in *Vhl* mutant mice is due to HIF-1 activation (because pVHL targets both HIF-1α and -2α for proteasomal degradation) (16), we further disrupted the Hif-1α gene in these mice thereby creating *Vhl*/*Hif-1α* double mutant mice (hS100A8-Cre + $Vhl^{fl/fl}$/$Hif\text{-}1\alpha^{fl/fl}$). *Vhl*/*Hif-1α* double mutant mice exhibited significantly reduced erythema (Fig. 2*A*) and decreased Vegf protein expression in the bone marrow lysate (Fig. 2*B*) compared with *Vhl* mutant mice. Significantly increased serum levels of Vegf in *Vhl* mutant mice were notably reduced in *Vhl*/*Hif-1α* double mutant mice and this level was similar to that in WT mice (Fig. 2*C*).

We then implanted matrigel in *Vhl* mutant mice and treated these animals with NSC 134754, an HIF-1 inhibitor (17). NSC 134754 significantly reduced CD31 area densities along with Hif-1α, Vegf, and S100A8 protein levels in matrigel (Fig. 2*D*). Matrigel implanted in *Vhl*/*Hif-1α* double mutant mice revealed very similar results (Fig. 2*D*), suggesting that neovascularization in matrigel in *Vhl* mutant mice was due to HIF-1 activation in myeloid cells.

To confirm that HIF-1, but not HIF-2, activation in myeloid cells drives blood vessel formation in matrigel, we further generated the myeloid-specific *Hif-1α* (hS100A8Cre + $Hif\text{-}1\alpha^{fl/fl}$), *Hif-2α* (hS100A8Cre + $Hif\text{-}2\alpha^{fl/fl}$), or *Hif-1α*/*Hif-2α* double (hS100A8Cre + $Hif\text{-}1\alpha^{fl/fl}$/$Hif\text{-}2\alpha^{fl/fl}$) mutant mice and implanted matrigel in these mice. We found that CD31 area densities were significantly reduced in *Hif-1α* mutant or *Hif-1α*/*Hif-2α* double mutant mice compared with their corresponding WT mice (Fig. 2*E*). On the other hand, CD31 area densities were comparable between *Hif-2α* mutant and WT mice (Fig. 2*E*). These results thus indicate that HIF-1, not HIF-2, activation in myeloid cells is a major determinant for blood vessel formation in matrigel. By performing the antibody array, we observed similar Vegf protein levels in bone marrow lysates of *Hif-1α* mutant and WT mice (Fig. S2*A* and Table S3).

Monocytes Are the Major Effector Responsible for HIF-1–Mediated VEGF and S100A8 Production. We first determined whether neovascularization in matrigel in *Vhl* mutant mice derived from bone marrow-derived cells. To do this, we performed bone marrow transplantation (BMT) in which WT mice were reconstituted with *Vhl* mutant (WT + *Vhl* BMT) or WT (WT + WT BMT) bone marrow cells, or *Vhl* mutant mice were reconstituted with

MEDICAL SCIENCES

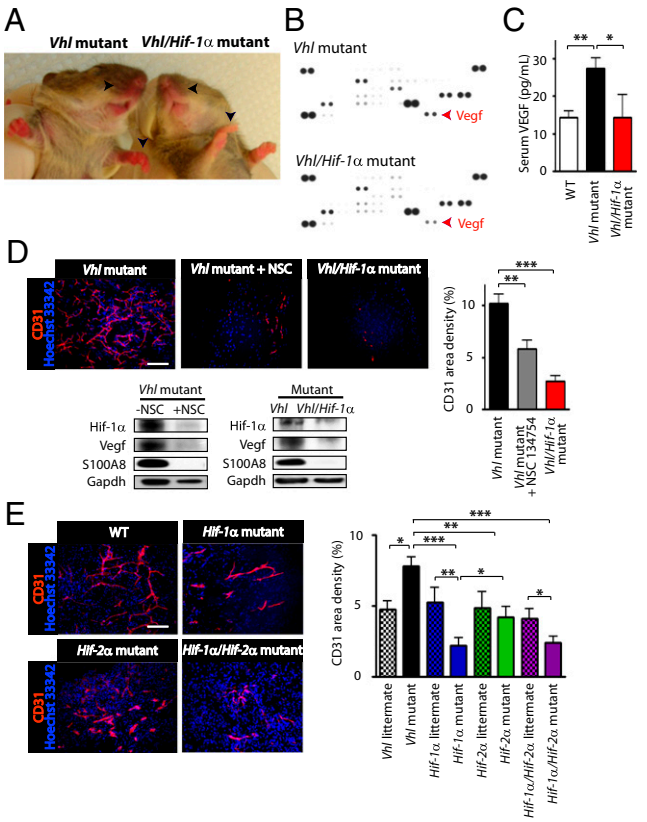

Fig. 2. Angiogenic phenotypes in mice deficient for pVHL in hS100A8 myeloid cells require HIF-1 activation. (*A*) Inactivation of *Hif-1α* in *Vhl* mutant mice (*Vhl/Hif-1α* mutant) suppressed erythema of *Vhl* single mutant mice (black arrowheads). (*B*) Antibody array analyses as in Fig. 1 for *Vhl* or the *Vhl/Hif-1α* mutant mice bone marrow lysates. Note that the increased Vegf in *Vhl* mutant mice is significantly reduced in *Vhl/Hif-1α* mutant mice (red arrowheads). (*C*) Serum VEGF measured by ELISA ($n = 5$ per group). (*D*) Immunostaining (*Upper*) and Western blots (*Lower*) of matrigel implanted in *Vhl* mutant mice, *Vhl* mutant mice treated with NSC 134754, a HIF-1 inhibitor, or in *Vhl/Hif-1α* mutant mice. (Scale bar: 100 μm.) Quantification of CD31 area density is shown in the bar graph ($n = 10$ for *Vhl* mutant; $n = 7$ for *Vhl* mutant + NSC; $n = 6$ for *Vhl/Hif-1α* mutant). (*E*) Immunostaining of matrigel implanted in WT, *Hif-1α* mutant, *Hif-2α* mutant, or *Hif-1α /Hif-2α* mutant mice. Quantification of CD31 area densities in matrigel is shown in the bar graph ($n = 7$ for *Vhl* littermate; $n = 7$ for *Vhl* mutant; $n = 6$ for *Hif-1α* littermate; $n = 10$ for *Hif-1α* mutant; $n = 4$ for *Hif-2α* littermate; $n = 6$ for *Hif-2α* mutant; $n = 5$ for *Hif-1α/Hif-2α* littermate; $n = 6$ for *Hif-1α/Hif-2α* mutant). In *C*, *D*, and *E*, data are the mean ± SEM and $*P < 0.05$, $**P < 0.01$, and $***P < 0.001$ determined by one-way ANOVA.

WT (*Vhl* + WT BMT) bone marrow cells. Four weeks later, we implanted matrigel in these mice and examined $CD31^+$ endothelial cells, as previously described. We observed that matrigel harvested from WT + *Vhl* BMT had significantly higher CD31 area densities, Hif-1α, and S100A8 protein levels compared with those from WT + WT BMT (Fig. 3). In contrast, *Vhl* + WT BMT exhibited significantly reduced CD31 area densities compared with WT + *Vhl* BMT (Fig. 3*B*), indicating that neovascularization in matrigel is driven by bone marrow-derived cells. CD11b area densities in matrigel were similar in all groups (Fig. 3*B*) and are consistent with our previous results without BMT (Fig. 1*F*).

The hS100A8 promoter is known to target various subsets of cells within the myeloid lineage (12). To identify which subset(s) of the myeloid cells was responsible for the angiogenic effects in *Vhl* mutant mice, we isolated myeloid subsets targeted by the hS100A8 promoter, namely common myeloid progenitors (CMPs), granulocyte-macrophage progenitors (GMPs), pregranulocytes (PreGs), granulocytes (Grs), and monocytes by FACS. Immunophenotyping analysis revealed that the frequency of each myeloid population did not differ between WT and *Vhl* mutant mice (Fig. 4*A* and Fig. S2*B*). The absolute numbers of whole bone marrow cells were also similar in these animals [WT mice, $(1.4 \pm 0.1) \times 10^7$ cells ($n = 4$); *Vhl* mutant mice, $(1.5 \pm 0.2) \times 10^7$ cells ($n = 4$)].

By performing quantitative real-time PCR (qRT-PCR) with 20,000 cells isolated from each subset, we found that the mRNA levels of Hif-1α and Vegf were significantly increased only in monocytes obtained from *Vhl* mutant mice (Fig. 4*B*). Consistent with this finding, other HIF-1 downstream target genes including *Glut-1* and *Pgk* were also increased only in monocytes of *Vhl* mutant mice (Fig. S2*C*). *Hif-2α* or *Epo* transcripts were not detectable in any of the myeloid populations of *Vhl* mutant mice examined. Vhl mRNA levels were low in PreGs, granulocytes, and monocytes of the *Vhl* mutant mice (Fig. 4*B*).

By performing Western blots using monocytes isolated by FACS, we confirmed that Hif-1α, Vegf, and S100A8 proteins were significantly increased in *Vhl* mutant mice, whereas these proteins were, in turn, significantly decreased in *Vhl/Hif-1α* double mutant mice (Fig. 4*C*). Together, these results suggest that monocytes mediate HIF-1–induced VEGF and S100A8 production.

VEGF and S100A8 Cooperatively Act to Promote Neovascularization. To further dissect the role of VEGF and S100A8 in monocytes, we inactivated the Vegf gene thereby generating *Vhl/Vegf* double mutant mice (hS100A8Cre + $Vhl^{fl/fl}/Vegf^{fl/fl}$), and implanted matrigel in these animals. To our surprise, we observed similar neovascularization in matrigels implanted in *Vhl/Vegf* double mutant mice compared with that in *Vhl* mutant mice (Fig. 5*A*). To further interrogate this finding, we sorted monocytes from *Vhl* or *Vhl/Vegf* double mutant mice and performed Western blot and qRT-PCR analyses. We found that although VEGF was efficiently inactivated in *Vhl/Vegf* double mutant mice, S100A8 expression in monocytes was similar between *Vhl/Vegf* dougle and *Vhl* mutant mice (Fig. 5*B*). Because we observed higher S100A8 protein expression in sorted monocytes of *Vhl* mutant mice compared with WT (Fig. 4*C*), we then measured serum S100A8 levels in these animals. We found that serum S100A8 was significantly higher in *Vhl* mutant mice than WT and that S100A8 remained elevated in *Vhl/Vegf* double mutant mice (Fig.

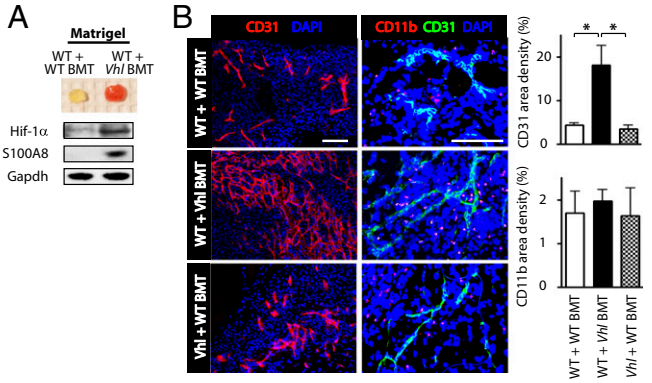

Fig. 3. Bone marrow-derived cells mediate neovascularization in matrigel. (*A*) A picture (*Upper*) and Western blots (*Lower*) of matrigel in WT mice reconstituted with WT bone marrow (WT + WT BMT, $n = 8$) or with *Vhl* mutant mice bone marrow (WT + *Vhl* BMT, $n = 8$). (*B*) Immunofluorescent staining of matrigels in WT + WT BMT, WT + *Vhl* BMT, or *Vhl* + WT BMT for CD31 or CD11b. Nuclei were counterstained by DAPI. (Scale bar: 100 μm.) Quantification of CD31 or CD11b area density is shown in the bar graphs. Data are the mean ± SEM with $*P < 0.05$ determined by one-way ANOVA ($n = 10$ for WT + WT BMT; $n = 8$ for WT + *Vhl* BMT; $n = 5$ for *Vhl* + WT BMT).

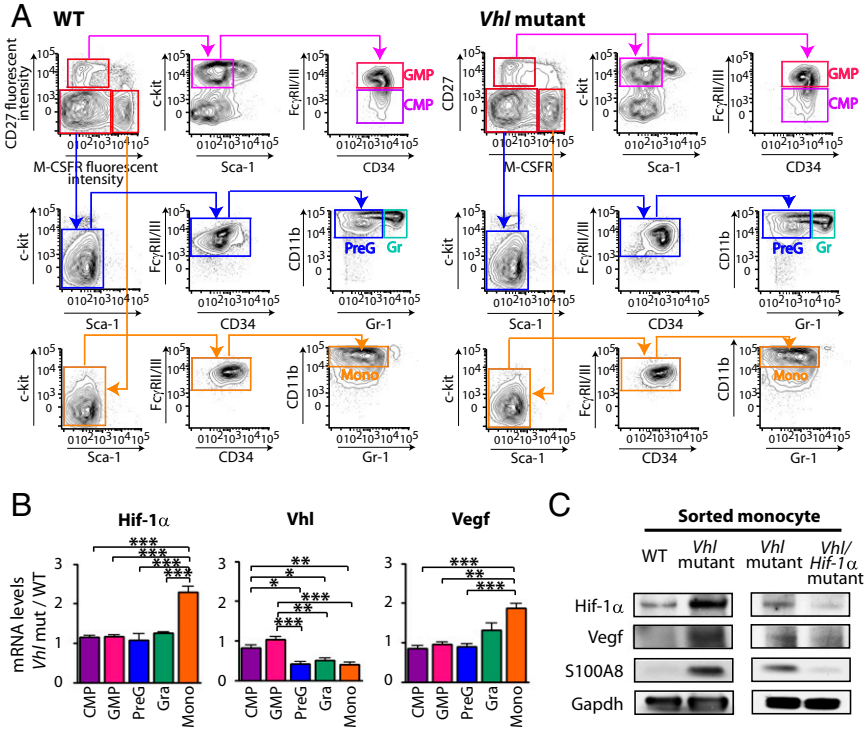

Fig. 4. Monocytes are the major effector mediating angiogenic effects. (*A*) Immunophenotyping analyses of CMPs, GMPs, PreGs, granulocytes (Gr), and monocytes (Mono) of WT or *Vhl* mutant mice. (*B*) qRT-PCR analyses in 20,000 cells sorted from each myeloid subpopulation for Hif-1α, Vhl, and Vegf. Results are quantified as fold changes of mRNA in *Vhl* mutant over WT mice. $*P < 0.05$, $**P < 0.01$, and $***P < 0.001$ determined by one-way ANOVA using triplicate determinations from pooled samples of two animals per group. Data are the mean ± SEM. (*C*) Western blots performed with FACS sorted monocytes obtained from WT, *Vhl* mutant, or *Vhl*/*Hif-1α* mutant mice.

5*B*). This is consistent with an increased gene expression of S100A8 in sorted monocytes of *Vhl* or *Vhl*/*Vegf* double mutant mice (Fig. S2*E*). To test the possibility whether S100A8 production is regulated by HIF-1, we measured serum S100A8 levels in *Vhl* or *Vhl*/*Hif-1α* double mutant mice and found that the elevated S100A8 in *Vhl* mutant was significantly reduced in *Vhl*/*Hif-1α* double mutant mice (Fig. 5*C*), indicating that HIF-1 regulates S100A8.

We then examined neovascularization efficiency of S100A8 in matrigel. To do this, we implanted matrigel in WT mice that had been supplemented with VEGF alone, S100A8 alone, or VEGF in combination with S100A8, all of which had been supplemented with bFGF. We observed that although S100A8 exhibited similar CD31 area densities to VEGF, when combined together with VEGF there was a significant increase in vessel formation in matrigel (Fig. 5*D*), and this level was comparable to that in *Vhl* mutant mice (Fig. 1*D*).

HIF-1–Activated Monocytes Promote Angiogenesis in Matrigel and Improve Blood Flow in a Mouse Model of Hindlimb Ischemia. To test whether HIF-1–activated monocytes are sufficient to promote neovascularization in vivo, we next sorted 100,000 monocytes from WT or *Vhl* mutant mice, admixed them directly with matrigel, and s.c. implanted in WT mice for 2 wk. We observed a profound level of neovascularization in matrigel admixed with *Vhl* mutant monocytes compared with that admixed with WT monocytes, whereas CD11b levels were similar (Fig. 6*A*).

We then investigated if HIF-1–activated monocytes can improve blood perfusion in a mouse model of hindlimb ischemia. To do this, we isolated 50,000 monocytes from WT or *Vhl* mutant mice by FACS, and injected them intramuscularly in the quadrate and adductor muscle of the thigh, and gastrocnemius muscle of WT animals 24 h after femoral artery ligation. We observed a significant improvement in blood flow of the ligated limb in mice injected with *Vhl* mutant monocytes compared with WT monocytes (Fig. 6*B*). Histology of the muscle at day 14 when the blood flow was maximally improved for both groups (Fig. 6*B* and Fig. S2*F*) revealed an increase in CD31 area densities in mice injected with *Vhl* mutant monocytes, whereas the CD11b area densities did not differ between *Vhl* mutant- and WT monocyte-injected groups (Fig. 6*C*). Overall these data indicate that transcriptional activation of HIF-1 in monocytes increases neovascularization in matrigel and improves blood flow in hindlimb ischemia in mice.

Discussion

Here we report our findings that transcriptional activation of HIF-1 in myeloid cells can promote angiogenesis by using our unique strain of myeloid-specific KO mice targeting HIF pathways. By inactivating pVHL in hS100A8 myeloid cells, we observed an erythema phenotype (Fig. 1*A*), enhanced blood vessel formation in matrigel (Fig. 1*D*), increased VEGF production in the bone marrow lysate (Fig. 1*C*), all of which were significantly suppressed by genetic or pharmacological inhibition of HIF-1 (Fig. 2), suggesting that HIF-1 is a major mediator in myeloid cells driving this effect. We further found that monocytes were the major effector in cells of the myeloid lineage for VEGF and S100A8 production (Fig. 4 *B* and *C*), promoting blood vessel formation in matrigel and improving blood flow in the mouse model of hindlimb ischemia (Fig. 6).

Despite the well-described myeloid-specific *HIF* KO mice of LysM promoter (10, 11), we did not observe the erythema phenotype in *Vhl* mutant mice using such a promoter (Fig. S1*A*). Furthermore, vessel formation in matrigel (Fig. S1*B*) and Hif-1α and Vegf protein levels in sorted monocytes (Fig. S1*G*) were similar between *Vhl* KO mice of LysM promoter and WT mice, suggesting that the LysM promoter may differ in efficiency of targeting subpopulations of myeloid cells. Indeed, the deletion efficiency of *Vhl* was approximately three times higher in monocytes of *Vhl* mutant mice using the hS100A8 promoter compared with the LysM promoter (Fig. S1*F*).

S100A8 expression is detected in fetal myeloid progenitors as early as at 11 d of gestation as well as immature myeloid cells in the bone marrow, myeloid cells in the splenic red pulp and marginal zone, and blood-borne monocytes and neutrophils in the adult mouse (12). The hS100A8 promoter has been previously

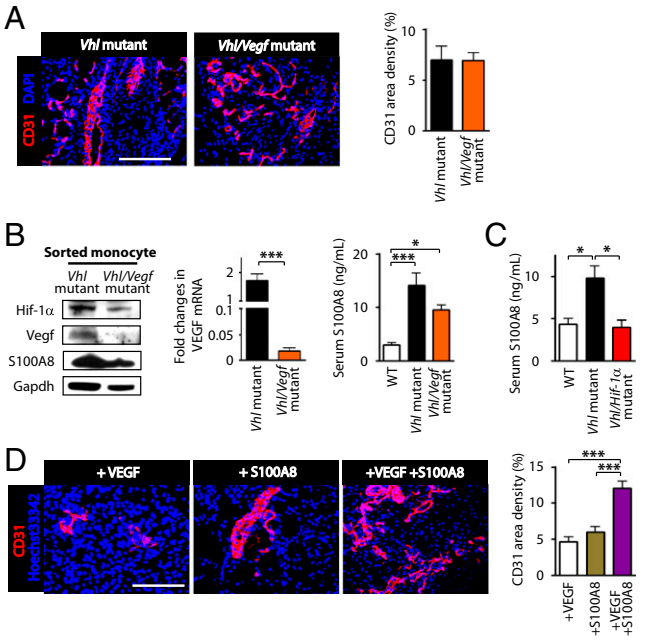

Fig. 5. VEGF and S100A8 act cooperatively to promote neovascularization in matrigel. (*A*) Matrigel immunostained for CD31 (red) implanted in *Vhl* mutant or *Vhl/Vegf* double mutant mice. Quantification of CD31 area densities are shown in the bar graph ($n = 5$ per group). (*B*) Western blot (*Left*) showing Hif-1α, Vegf, S100A8 protein levels in sorted monocytes obtained from *Vhl* or *Vhl/Vegf* mutant mice. qRT-PCR for Vegf (*Center*) was performed in these mice and quantified as fold changes compared with WT mice. $***P < 0.001$ by unpaired Student *t* test. Serum S100A8 levels (*Right*) in WT, *Vhl* mutant, or *Vhl/Vegf* mutant mice. $*P < 0.05$ and $***P < 0.001$, respectively, determined by one-way ANOVA ($n = 6$ per group). (*C*) Serum S100A8 measured in WT, *Vhl* mutant, or *Vhl/Hif-1α* mutant mice. $*P < 0.05$ ($n = 5$ per group). (*D*) Immunostaining of matrigel implanted in WT that had been admixed with VEGF alone, S100A8 alone, or VEGF in combination with S100A8. $***P < 0.001$ determined by one-way ANOVA ($n = 5$ per group). (Scale bars: 100 μm in *A* and *D*.) Data in *A–D* are the mean ± SEM.

used by other investigators and shown to successfully target cells in the myeloid lineage creating mouse models of acute myeloid leukemia (18, 19), which faithfully mimicked the human disease in mice.

Known as the endogenous Toll-like receptor 4 agonist (20), S100A8 has been shown to be regulated by glucocorticoids upon LPS stimulation (21). In our study, we found that transcriptional activation of HIF-1 in myeloid cells regulates S100A8 (Fig. 4*C*). Indeed a couple of recent reports have demonstrated that the hypoxia-independent stabilization of HIF-1α in mouse epidermis resulted in a dramatic increase in S100A8 gene expression (22) and that the S100A8 promoter contains HRE at the promoter sequence upstream of the transcription start site where HIF-1 binds and transcriptionally activates S100A8 expression (23).

Although the role of S100A8 in inflammation is extensively documented (24), its role in angiogenesis is still poorly understood. It has been demonstrated that S100A8 is secreted by myeloid cells (25) and that prerequisite for its secretion is the contact of myeloid cells with an inflamed endothelium (26) via heparin sulfate proteoglycans (27). Whereas low concentrations of S100A8 (10 ~ 25 μg/mL) have shown to promote migration and proliferation of endothelial cells (28) and increased vascular permeability (25), higher concentrations of S100A8 (200 μg/mL) have shown to result in endothelial apoptosis (29). Other mechanisms including S100A8/9-mediated increase in the binding capacity of CD11b/CD18 myeloid cells onto the endothelium (30) or nitric oxide production in myeloid cells (31) leading to vasodilation may also participate in S100A8 myeloid cell-driven angiogenesis.

HIF-1α and -2 α, being extensively characterized for their tight regulation by molecular oxygen via posttranslational modification (32). Previously published studies using primary human macrophages have demonstrated that in normoxic macrophages HIF-2α but not HIF-1α plays a dominant role in regulating *VEGF* transcription (33) whereas hypoxic macrophages rely on both HIF-1α and -2α for VEGF expression (34). This is in contrast to our study where we detected a significant increase in *Vegf* and *Glut-1* transcripts, but no detectable levels of *Hif-2α* or *Epo* transcripts in monocytes of our myeloid-specific *Vhl* KO mice (Fig. 4*B*), indicating HIF-1 predominance in our model system. It is possible that the difference in subsets of myeloid lineage (macrophage vs. monocytes) or technologies of gene expression (transfection vs. somatic gene deletion) could have contributed to this discrepancy.

Chronic critical limb ischemia (CLI) is characterized by marked hypoperfusion of the affected limb, often secondary to multilevel, atherosclerotic occlusive disease in humans (35). Although many attempts have been made to restore the blood

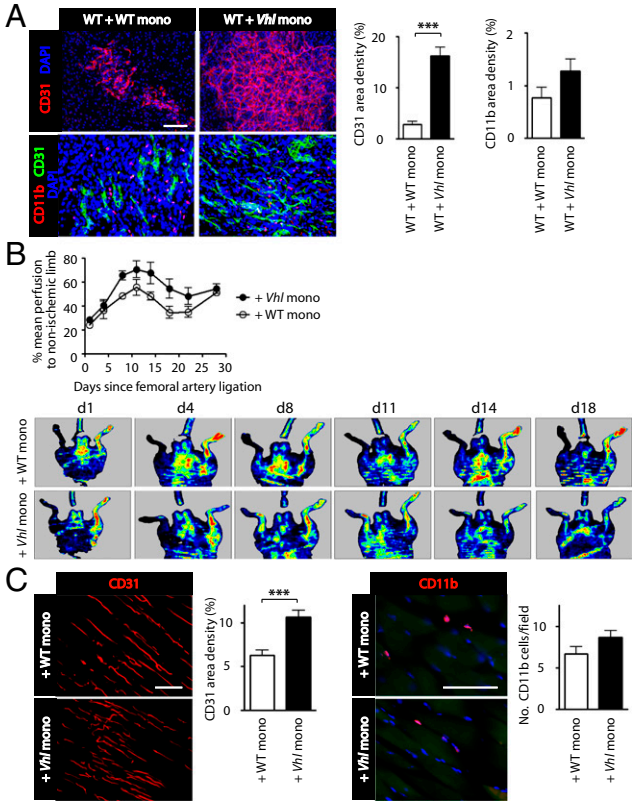

Fig. 6. HIF-1–activated monocytes promote angiogenesis in matrigel and improve blood flow in a mouse model of hindlimb ischemia. (*A*) Immunostaining of matrigel implanted in WT mice that had been admixed with 100,000 monocytes isolated from WT (WT mono) or *Vhl* mutant (*Vhl* mono) mice for CD31 and CD11b. (Scale bar: 100 μm.) Area densities of CD31 and CD11b in matrigel are shown (*Right*). $***P < 0.001$ determined by Student *t* test ($n = 6$ per group). (*B*) Laser Doppler flowmetry analysis of the blood perfusion in the femoral artery ligated WT animals injected intramuscularly with 50,000 monocytes isolated from WT mice (WT + WT mono) or *Vhl* mutant mice (WT + *Vhl* mono). The data are the mean ± SEM ($n = 6$ for WT + WT mono; $n = 7$ for WT + *Vhl* mono). Representative laser Doppler image from each group is shown (*Lower*). (*C*) Immunostaining of the quadrate muscle at day 14 for CD31 (*Left*) or CD11b (*Right*). $***P < 0.001$ determined by unpaired Student *t* test. (Scale bars: 100 μm.) Data in *A–C* are the mean ± SEM.

flow and improve tissue perfusion in patients with CLI (35), the therapeutic outcomes have been largely mixed. Recently, autologous bone marrow-derived mononuclear cell transplantation has been identified as a potential new therapeutic option to induce therapeutic angiogenesis and there are large randomized, placebo-controlled, double-blind studies taking place [bone marrow outcomes trial in critical limb ischemia (BONMOTCLI), rejuvenating endothelial progenitor cells via transcutaneous intra-arterial supplementation (JUVENTAS), and national clinical trial number (NCT) 00498069] to evaluate such strategy in patients with CLI (36). Based on our results, an ex vivo approach of transcriptional activation of HIF-1 in bone marrow-derived monocytes followed by autologous transplantation of these cells to the affected limb may also offer a highly attractive means to improve blood flow in CLI patients.

In summary, we report that HIF-1 activation in myeloid cells, mainly monocytes, promotes angiogenesis through VEGF and S100A8 production. Our study thus implies that HIF-1 activation in myeloid cells may offer a unique therapeutic strategy to treat diseases of abnormal vascularity such diabetic wounds.

Materials and Methods

Cre-mediated inactivation of pVHL, HIF-1α, or HIF-2α in myeloid cells was accomplished by generating mice that were homozygous for the respective 2-lox alleles as described elsewhere (16). In brief, we cross-bred mice having lox-P flanking alleles in *HIF-1α* (*Hif-1α*$^{fl/fl}$), *HIF-2α* (*Hif-2α*$^{fl/fl}$), or *von Hippel–Lindau* (*Vhl*$^{fl/fl}$), with transgenic mice bearing the *Cre-recombinase* gene under the hS100A8 or lysozyme (LysM) promoter. *Hif-1α*$^{fl/fl}$, *Hif-2α*$^{fl/fl}$, *Vhl*$^{fl/fl}$, and LysM-Cre mice were purchased from Jackson Laboratories and hS100A8Cre mice were obtained from I.L.W. (37). Additional information is available in *SI Materials and Methods*.

ACKNOWLEDGMENTS. We thank Dr. J. Ernst, Ms. J. Kirk, and B. Thompson, and other members on the Research and Development (R&D) Systems, Inc. Proteome Profiler Array development team for assistance with array image analysis. We also thank members at the animal facilities [Stanford University and Pohang University of Science and Technology (POSTECH)] and Ms. Hye-Jin Jung (FACS Core Facility). Special thanks go to Dr. Napoleone Ferrara (University of California, San Diego and Genetech) for generously providing the *VEGF* floxed mice. And finally we thank Drs. Seung-Jae Lee (POSTECH) and Volker H. Haase (Vanderbilt University) for their helpful technical advice. Y.-E.K. [National Research Foundation (NRF)-2012H1A2A1002871] and B.-J.H. (NRF-2013H1A2A1032808) are Global Ph.D. Fellows. This study was supported by NRF-2012R1A1A3010225, NRF-2012M2B2B1055641, and NRF-2012M3A9C6049796 (to G-O.A.), and 2013R1A1A1007199 (to H.J.K.) from the Ministry of Science, Information, Communication, Technology, and Future Planning Korea; National R&D Program for Cancer Control (Grant 1320220 to G-O.A.) from National Cancer Center Korea; BK21 Plus (10Z20130012243) by the Ministry of Education Korea; and National Institutes of Health Grants U01HL099999 (to I.L.W.) and CA149318 (to J.M.B.).

1. Lamalice L, Le Boeuf F, Huot J (2007) Endothelial cell migration during angiogenesis. *Circ Res* 100(6):782–794.
2. Granata F, et al. (2010) Production of vascular endothelial growth factors from human lung macrophages induced by group IIA and group X secreted phospholipases A2. *J Immunol* 184(9):5232–5241.
3. Medina RJ, et al. (2011) Myeloid angiogenic cells act as alternative M2 macrophages and modulate angiogenesis through interleukin-8. *Mol Med* 17(9-10):1045–1055.
4. Kujawski M, et al. (2008) Stat3 mediates myeloid cell-dependent tumor angiogenesis in mice. *J Clin Invest* 118(10):3367–3377.
5. Shojaei F, Zhong C, Wu X, Yu L, Ferrara N (2008) Role of myeloid cells in tumor angiogenesis and growth. *Trends Cell Biol* 18(8):372–378.
6. Semenza GL (2003) Targeting HIF-1 for cancer therapy. *Nat Rev Cancer* 3(10):721–732.
7. Kim KS, Rajagopal V, Gonsalves C, Johnson C, Kalra VK (2006) A novel role of hypoxia-inducible factor in cobalt chloride- and hypoxia-mediated expression of IL-8 chemokine in human endothelial cells. *J Immunol* 177(10):7211–7224.
8. Calvani M, Rapisarda A, Uranchimeg B, Shoemaker RH, Melillo G (2006) Hypoxic induction of an HIF-1alpha-dependent bFGF autocrine loop drives angiogenesis in human endothelial cells. *Blood* 107(7):2705–2712.
9. Haase VH (2010) Hypoxic regulation of erythropoiesis and iron metabolism. *Am J Physiol Renal Physiol* 299(1):F1–F13.
10. Cramer T, et al. (2003) HIF-1alpha is essential for myeloid cell-mediated inflammation. *Cell* 112(5):645–657.
11. Imtiyaz HZ, et al. (2010) Hypoxia-inducible factor 2alpha regulates macrophage function in mouse models of acute and tumor inflammation. *J Clin Invest* 120(8):2699–2714.
12. Lagasse E, Weissman IL (1992) Mouse MRP8 and MRP14, two intracellular calcium-binding proteins associated with the development of the myeloid lineage. *Blood* 79(8):1907–1915.
13. Clausen BE, Burkhardt C, Reith W, Renkawitz R, Förster I (1999) Conditional gene targeting in macrophages and granulocytes using LysMcre mice. *Transgenic Res* 8(4):265–277.
14. Purhonen S, et al. (2008) Bone marrow-derived circulating endothelial precursors do not contribute to vascular endothelium and are not needed for tumor growth. *Proc Natl Acad Sci USA* 105(18):6620–6625.
15. Shibuya M (2006) Differential roles of vascular endothelial growth factor receptor-1 and receptor-2 in angiogenesis. *J Biochem Mol Biol* 39(5):469–478.
16. Haase VH (2006) Hypoxia-inducible factors in the kidney. *Am J Physiol Renal Physiol* 291(2):F271–F281.
17. Chau N-M, et al. (2005) Identification of novel small molecule inhibitors of hypoxia-inducible factor-1 that differentially block hypoxia-inducible factor-1 activity and hypoxia-inducible factor-1alpha induction in response to hypoxic stress and growth factors. *Cancer Res* 65(11):4918–4928.
18. Jaiswal S, et al. (2003) Expression of BCR/ABL and BCL-2 in myeloid progenitors leads to myeloid leukemias. *Proc Natl Acad Sci USA* 100(17):10002–10007.
19. Yuan Y, et al. (2001) AML1-ETO expression is directly involved in the development of acute myeloid leukemia in the presence of additional mutations. *Proc Natl Acad Sci USA* 98(18):10398–10403.
20. Ehrchen JM, Sunderkötter C, Foell D, Vogl T, Roth J (2009) The endogenous Toll-like receptor 4 agonist S100A8/S100A9 (calprotectin) as innate amplifier of infection, autoimmunity, and cancer. *J Leukoc Biol* 86(3):557–566.
21. Hsu K, et al. (2005) Regulation of S100A8 by glucocorticoids. *J Immunol* 174(4):2318–2326.
22. Wondimu A, et al. (2012) Loss of Arnt (Hif1β) in mouse epidermis triggers dermal angiogenesis, blood vessel dilation and clotting defects. *Lab Invest* 92(1):110–124.
23. Grebhardt S, Veltkamp C, Ströbel P, Mayer D (2012) Hypoxia and HIF-1 increase S100A8 and S100A9 expression in prostate cancer. *Int J Cancer* 131(12):2785–2794.
24. Ryckman C, Vandal K, Rouleau P, Talbot M, Tessier PA (2003) Proinflammatory activities of S100: Proteins S100A8, S100A9, and S100A8/A9 induce neutrophil chemotaxis and adhesion. *J Immunol* 170(6):3233–3242.
25. Viemann D, et al. (2005) Myeloid-related proteins 8 and 14 induce a specific inflammatory response in human microvascular endothelial cells. *Blood* 105(7):2955–2962.
26. Frosch M, et al. (2000) Myeloid-related proteins 8 and 14 are specifically secreted during interaction of phagocytes and activated endothelium and are useful markers for monitoring disease activity in pauciarticular-onset juvenile rheumatoid arthritis. *Arthritis Rheum* 43(3):628–637.
27. Robinson MJ, Tessier P, Poulsom R, Hogg N (2002) The S100 family heterodimer, MRP-8/14, binds with high affinity to heparin and heparan sulfate glycosaminoglycans on endothelial cells. *J Biol Chem* 277(5):3658–3665.
28. Li C, et al. (2012) Low concentration of S100A8/9 promotes angiogenesis-related activity of vascular endothelial cells: Bridges among inflammation, angiogenesis, and tumorigenesis? *Mediators Inflamm* 2012:248574.
29. Viemann D, et al. (2007) MRP8/MRP14 impairs endothelial integrity and induces a caspase-dependent and -independent cell death program. *Blood* 109(6):2453–2460.
30. Newton RA, Hogg N (1998) The human S100 protein MRP-14 is a novel activator of the beta 2 integrin Mac-1 on neutrophils. *J Immunol* 160(3):1427–1435.
31. Pouliot P, Plante I, Raquil M-A, Tessier PA, Olivier M (2008) Myeloid-related proteins rapidly modulate macrophage nitric oxide production during innate immune response. *J Immunol* 181(5):3595–3601.
32. Weidemann A, Johnson RS (2008) Biology of HIF-1alpha. *Cell Death Differ* 15(4):621–627.
33. White JR, et al. (2004) Genetic amplification of the transcriptional response to hypoxia as a novel means of identifying regulators of angiogenesis. *Genomics* 83(1):1–8.
34. Fang HY, et al. (2009) Hypoxia-inducible factors 1 and 2 are important transcriptional effectors in primary macrophages experiencing hypoxia. *Blood* 114(4):844–859.
35. Mohler ER, 3rd, et al. (2003) Adenoviral-mediated gene transfer of vascular endothelial growth factor in critical limb ischemia: Safety results from a phase I trial. *Vasc Med* 8(1):9–13.
36. Lawall H, Bramlage P, Amann B (2010) Stem cell and progenitor cell therapy in peripheral artery disease. A critical appraisal. *Thromb Haemost* 103(4):696–709.
37. Passegué E, Wagner EF, Weissman IL (2004) JunB deficiency leads to a myeloproliferative disorder arising from hematopoietic stem cells. *Cell* 119(3):431–443.